






Circulating large extracellular vesicles as diagnostic biomarkers of indeterminate thyroid nodules: multi-platform omics analysis

Nada M. Ahmed^{1,2} , Mohammad M. R. Eddama^{3,*} , Kevin Beatson³ , Rijan Gurung³, Jigisha Patel³, Georges Iskandar⁴, Alaa Abdel-Salam⁵ , Abdullah Al-Omar⁵, Richard Cohen³, Tarek Abdel-Aziz⁵  and Lucie Clapp¹

¹Institute of Cardiovascular Sciences, University College London, London, UK

²Pathology Department, Alexandria University, Alexandria, Egypt

³Department of Surgical Biotechnology, Division of Surgery and Interventional Science, University College London, London, UK

⁴Department of Anaesthesia and Perioperative Medicine, University College London Hospitals, London, UK

⁵Endocrine Surgery Unit, University College London Hospitals, London, UK

*Correspondence to: Mohammad M. R. Eddama, Research Department of Surgical Biotechnology, University College London, GI Services, Ground Floor, 250 Euston Road, London NW1 2PG, UK (e-mail: m.eddama.12@ucl.ac.uk)

Abstract

Background: While most thyroid nodules are benign, 7–15% are malignant. Patients with indeterminate thyroid nodules (specifically Bethesda IV/Thy3f) often undergo diagnostic hemithyroidectomy to reach a diagnosis on final histology. The aim of this study was to assess the feasibility of circulating large extracellular vesicles as diagnostic biomarkers in patients presenting with Thy3f thyroid nodules.

Methods: This was a two-gate diagnostic accuracy study; patients with Thy3f thyroid nodules were age, sex and body mass index matched to healthy individuals. Final histology confirmed benign and malignant diagnoses. Plasma large extracellular vesicle counts were quantified using flow cytometry. Large extracellular vesicle microRNA and protein profiles were identified using next generation sequencing and mass spectrometry, respectively.

Results: A total of 42 patients with Thy3f nodules (22 with cancer, 20 with non-cancer diagnosis) and 16 healthy controls were included. Total large extracellular vesicle concentrations and the concentrations of extracellular vesicles expressing epithelial cell adhesion molecule and the cancer markers atypical chemokine receptor type 7, extracellular matrix metalloproteinase inducer and syndecan-4 were significantly higher in patients with Thy3f nodules (cancer and non-cancer) compared with healthy individuals. In patients with cancerous versus non-cancer Thy3f nodules, one microRNA was upregulated: mir-195-3p ($P < 0.001$). Five were downregulated: mir-3176 ($P < 0.001$), mir-205-5p ($P < 0.001$), novel-hsa-mir-208-3p ($P < 0.001$), mir-3529-3p ($P = 0.01$) and let-7i-3p ($P = 0.02$). Furthermore, three large extracellular vesicle proteins (kallikrein-related peptidase11 (KLK11) ($P = 0.001$), alpha-1-acid glycoprotein 2 (A1AG2) ($P < 0.001$) and small integral membrane protein 1 (SMIM1) ($P = 0.04$)) were significantly upregulated, while 20 large extracellular vesicle proteins were significantly downregulated (most downregulated: chemokine (C-X-C motif) ligand 7 (CXCL7), tubulin beta chain 1 (TBB1), binding immunoglobulin protein (BIP) and actinin alpha 1 (ACTN1) ($P < 0.001$)) in cancerous compared with non-cancer Thy3f nodules.

Conclusion: Circulating large extracellular vesicle miRNA and protein profiles have a high diagnostic value to discriminate between benign and malignant nodules for patients with Thy3f cytology. Further validation for clinical performance will be needed.

Introduction

Thyroid cancer incidence has increased three-fold over the past four decades and now has the seventh highest cancer incidence globally. Thyroid nodules are largely benign, however, 7–15% will be malignant depending on factors such as age, sex, radiation exposure and family history¹. Clinical assessment, imaging and cytology can establish a diagnosis in approximately 80% of nodules²; the remaining 20% are categorized as 'indeterminate'³. Specifically, the category of Thy3f in the Royal College of Pathology system⁴ (known as Bethesda IV in the American system²) carries 15–30% risk of malignancy^{2,5}. Currently, patients with a cytological diagnosis of Thy3f are offered diagnostic hemithyroidectomy to confirm histological

diagnosis. Hemithyroidectomy carries risks of metabolic and anatomic surgical complications and the potential need for lifelong thyroid hormone supplementation, impacting patient productivity and quality of life⁶. There is an urgent need for a non-invasive diagnostic test to distinguish malignant from benign Thy3f nodules without the need for diagnostic surgery.

There are currently molecular tests designed to stratify risk on cytology. These include ThyroSeq version 3, Genomic Classifier, Afirma Gene Sequencing Classifier and Xpression Atlas, and combined ThyGeNEXT and ThyraMIR¹. Despite advances, clinical applicability is hindered by cost, low predictive value, the invasive nature of cytological sampling and lack of Food and Drug Association (FDA) and National Institute for Health and Care Excellence (NICE) approvals^{5,7}.

Received: July 08, 2024. Revised: October 02, 2024. Accepted: October 08, 2024

© The Author(s) 2024. Published by Oxford University Press on behalf of BJS Foundation Ltd.

This is an Open Access article distributed under the terms of the Creative Commons Attribution License (<https://creativecommons.org/licenses/by/4.0/>), which permits unrestricted reuse, distribution, and reproduction in any medium, provided the original work is properly cited.

Liquid biopsy is a non-invasive method involving the analysis of molecular alterations of cancer from tumour-derived components in body fluids, such as blood⁸. One blood component showing great promise as biomarkers are extracellular vesicles (EVs). These are anucleate nanosized vesicles bound by a phospholipid bilayer membrane. EVs are shed from body cells, including tumour cells, into the extracellular space and subsequently into blood. This shedding increases when cells undergo proliferation, cell division or apoptosis⁹.

Microvesicles or large EVs (L-EVs, 100–1000 nm) are a subset of EVs that bud directly from the cell membrane and play a role in intercellular communication¹⁰. They express membrane receptors and contain bioactive cargo including RNA, DNA and proteins that originate from their parent cells¹¹. There are advantages of EVs over other blood biomarkers. First, EVs are typically produced in greater quantities compared with other biomarkers like circulating tumour cells and circulating DNA. This is especially important in cancers producing low quantities of these other markers, resulting in low detection rates, as is the case in differentiated thyroid cancers¹². Second, EV biomarkers are stable as their vesicular membrane protects their contents¹³. For example, EV-enclosed RNAs are shielded from blood-derived RNases, preventing their degradation¹⁴.

To this end, transcriptomics and proteomics to characterize EV biomarkers are novel high-throughput approaches to quantify RNA and protein composition. These accelerate biomarker discovery and are gaining traction for biomarker development for many diseases, including cancer¹⁵.

The aims of this study were to assess circulating L-EV counts through a non-invasive blood test, analyse their membrane surface markers and utilize multi-platform omics to identify potential diagnostic L-EV biomarkers capable of distinguishing between benign and malignant Thy3f nodules.

Methods

Patient recruitment and ethical approval

This study adopted a mixed design including a two-gate diagnostic case-control design, using healthy control participants (HCs) and a single-gate classic design for patients with Thy3f nodules. Patients with Thy3f nodules underwent hemithyroidectomy at University College London Hospital between October 2020 and October 2023. HCs were age, sex and body mass index matched and recruited from staff members at University College London. HCs were not on regular medications, not known to suffer from any health conditions and had no symptoms of thyroid disease. Excluded were: children below the age of 18 years, patients with other active cancer or inflammatory conditions and those with acute illnesses. Patient demographics were collected using the hospital electronic health record system (EPIC: 2020 EPIC system Corporation, Verona, USA). All study participants provided written informed consent. This study received ethical approval by the Health Research Authority and Health and Care Research Wales (REC reference 21/NW/0023 and UCL-RFH).

Blood sample collection, L-EV isolation and characterization from plasma

Blood samples were collected in lavender EDTA vacutainer tubes (BD, Oxford, UK) from Thy3f patients after an overnight fast, immediately before undergoing surgery and before the induction of anaesthesia. Blood samples from HCs were similarly collected after an overnight fast. Within 2 h of blood draw, platelet poor

plasma (PPP) was obtained by double centrifugation: first at 56,112 r.p.m./2,350 rcf for 10 min to obtain plasma, then 81,966 r.p.m./5,000 rcf for 10 min to deplete platelets (MIBlood EV checklist¹⁶ with details of blood handling for L-EV isolation are in [Supplementary file S2](#)). PPP was aliquoted then stored at –80°C until analysis. L-EVs were isolated by differential centrifugation, size exclusion chromatography (SEC) or the Qiagen ExoRNEasy midi kit (Qiagen, Venlo, Netherlands) for analysis by flow cytometry, mass spectrometry and microRNA (miRNA) sequencing respectively. L-EV morphology and size distribution were assessed by transmission electron microscopy ([Fig. 1a](#)) and nanoparticle tracking analysis ([Supplementary file S1, Fig. S5](#)) respectively. The potential lipoprotein contamination level was measured by western blotting using anti-apolipoprotein B ([Supplementary file S1, Fig. S7](#)).

Measurement of L-EV surface markers by flow cytometry

L-EVs were analysed using a scatter calibrated Cytoflex S flow cytometer (Beckman Coulter, USA) with violet (405 nm laser) side scatter. The size gate was set between approximately 210 (limit of detection) to 1000 nm. L-EVs expressing the anionic phospholipid phosphatidylserine were labelled with the generic EV marker lactadherin conjugated to fluorescein isothiocyanate (FITC) (BLAC-FITC, Prolytix, Vermont, USA)¹⁷. L-EVs positive for lactadherin and within size range 210–1000 nm were assessed for positivity to different surface protein markers by incubation with appropriate antibody-fluorophore conjugates ([Fig. 1b](#)). EpCAM-BV421 was studied as an epithelial marker, while surface cancer markers analysed were atypical chemokine receptor type 7 conjugated to phycoerythrin (CXCR7-PE), extracellular matrix metalloproteinase inducer conjugated to brilliant violet 421 (CD147-BV421) and syndecan-4 conjugated to allophycocyanin (SDC4-APC). Antibodies were purchased from BD Biosciences, USA, except for SDC4 which was from R&D (Bio-Techne, Abingdon, UK). Detailed L-EV flow cytometry methods and the MIFlowCyt-EV guidelines¹⁸ checklist are in [Supplementary file S1, Fig. S2](#).

L-EV miRNA profiling by next generation sequencing

Plasma L-EVs from six non-cancer patients (two hyperplastic nodules, three follicular adenomas, one non-invasive follicular thyroid neoplasm with papillary like nuclear features (NIFTP)), eight cancer patients (five follicular variant of papillary thyroid carcinoma (FV-PTC), one mixed classic and FV-PTC, two follicular thyroid carcinoma (FTC)), and three age, sex and BMI matched HCs (pooled from seven HCs) were sequenced. The integrity and concentration of RNA were assessed using an Agilent 2100 Bioanalyzer (Agilent technologies, USA) ([Fig. S3](#)). BGI Genomics performed miRNA library preparation using an in-house kit and next generation sequencing (NGS) was performed on the DNBSEQ-G400 platform (BGI, Hong Kong). Reads were aligned to the reference genome: Homo_sapiens_UCSC_hg38 (RefSeq & Gencode gene annotations)¹⁹.

L-EV proteome profiling by liquid chromatography/mass spectrometry

After L-EV isolation by a combination of differential centrifugation and SEC, L-EV-rich fractions with minimal plasma protein contamination were identified by flow cytometry and total protein measurements using the BCA Protein Assay Kit (23227, Thermofisher Scientific, USA) (details in [Supplementary](#)

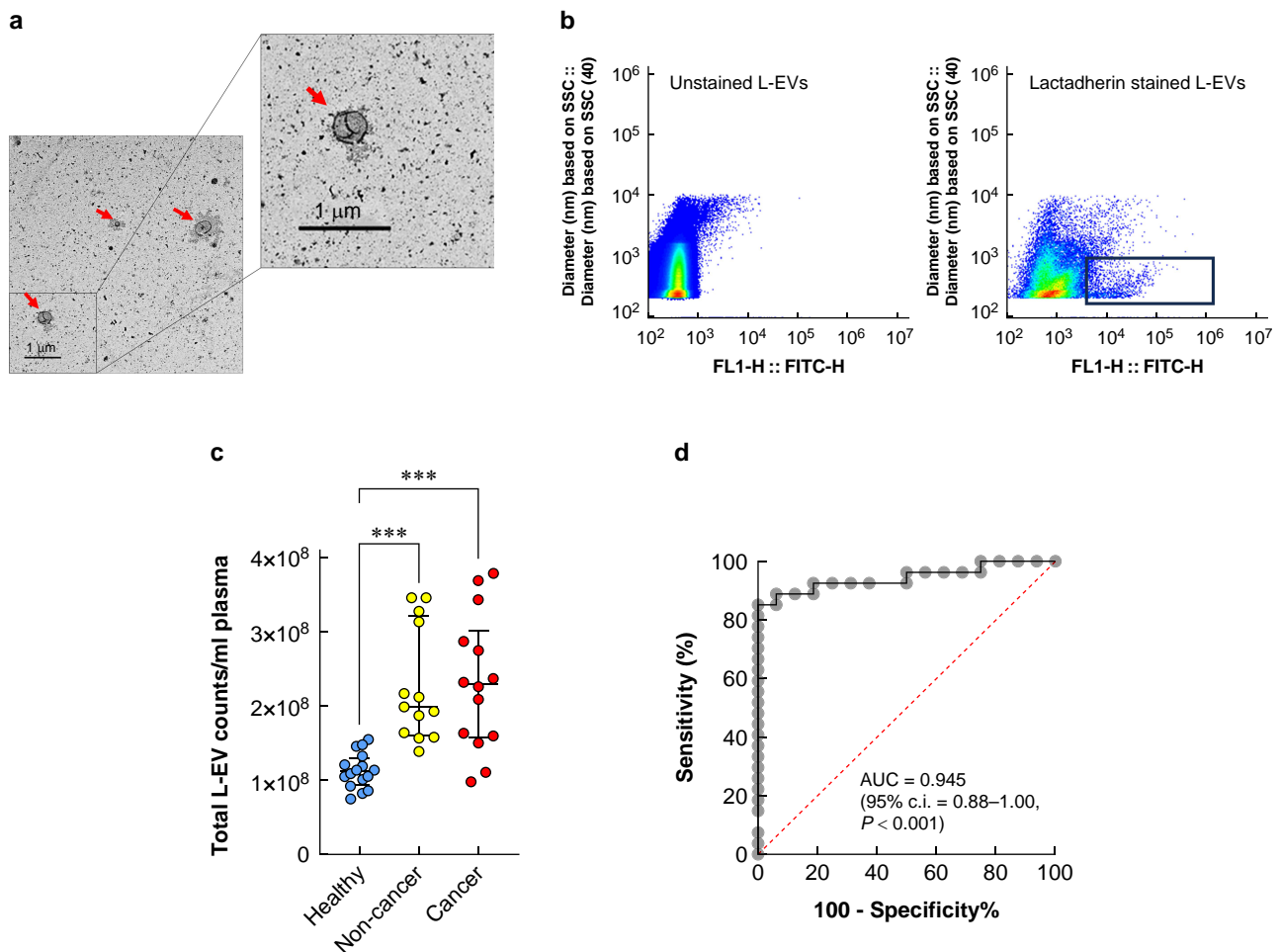


Fig. 1 Total L-EV concentrations are elevated in plasma of patients with indeterminate Thy3f thyroid nodules compared with healthy controls

a Transmission electron microscopy images demonstrating the morphology and size of L-EVs (100–1000 nm). **b** Pseudocolour plot of unstained (left) and lactadherin-FITC stained (right) L-EV samples; calibrated violet side scatter on the y-axis (diameter in nanometres) and FITC-H on the x-axis (arbitrary flow cytometry units). A size gate ranging from the limit of detection around 210 nm to an upper boundary of 1 μ m. **c** The concentration of total plasma L-EV counts stained with lactadherin-FITC. Healthy controls ($n=16$): blue circles, non-cancer Thy3f nodules: ($n=14$) yellow circles and cancer Thy3f nodules: ($n=14$) red circles. **d** A receiver operator curve (ROC) analysis of total lactadherin-FITC staining L-EV concentrations in indeterminate Thy3f thyroid nodules compared with healthy controls. Area under the curve (AUC) of 0.945 (95% c.i. 0.88–1.00, $P=0.001$). Statistical analysis was tested using the Kruskal–Wallis test. Statistical significance was set at $P\leq 0.05$ (two-sided). Data are presented as median and interquartile ranges. *** $P<0.001$. SSC, side scatter; L-EV, large extracellular vesicle; FITC, fluorescein isothiocyanate.

file S1, Fig. S4). Plasma L-EVs from 12 non-cancer Thy3f patients (5 hyperplastic nodules, 4 follicular adenomas, 3 NIFTPs), 12 cancer patients (6 FV-PTC, 3 mixed classic and FV-PTC, 3 FTC), and ten age, sex and BMI matched HCs were digested by trypsin and prepared for label-free quantification liquid chromatography/mass spectrometry (LC/MS). Samples were analysed in duplicate on a Bruker timsTOF Pro mass spectrometer connected to an Evosep One liquid chromatography system (Evosep, Denmark) as detailed in [Supplementary file S1](#). Raw data was searched against the *Homo sapiens* subset of the Uniprot Swissprot database. We have submitted all relevant data of our experiments to the EV-TRACK knowledgebase (EV-TRACK ID: EV240166)²⁰.

Statistical analysis

Data were analysed using GraphPad Prism version 10 (GraphPad Software, San Diego, CA, USA). Depending on data distribution, data were expressed as median and interquartile range if not normally distributed or mean and standard deviation if normally distributed. For inference statistics, t test, ANOVA or their non-parametric alternatives were used to analyse continuous data

as appropriate. The chi-square test was used to analyse categorical data. Receiver operating characteristic (ROC) curve and area under the curve (AUC) analyses were used to establish the diagnostic accuracy of L-EVs. Statistical significance was regarded when P value ≤ 0.05 (two-sided). For NGS data, expression of miRNAs was compared between patients with cancer, non-cancer nodules and HCs using DeSeq2 software on the Dr Tom bioinformatics data analysis portal (BGI, Hong Kong). Mass spectrometry data was analysed by GraphPad Prism and Perseus software²¹ and Venn diagrams created in Venny²². Significant differential expression of miRNAs and proteins was set at $P\leq 0.05$ and a log2 fold change threshold $-1 > \log_2\text{FC} > 1$ ²³. An *a priori* power calculation was not possible since this is, to our knowledge, the first study looking at L-EVs as diagnostic biomarkers for Thy3f nodules. Post-hoc power calculation for L-EV counts from flow cytometry were conducted and the statistical power was more than 95% for total L-EV counts performed using G*Power (version 3.1, website: <http://www.gpower.hhu.de/>).

For dichotomizing Thy3f diagnoses, the low-risk tumour NIFTPs were analysed in the non-cancer arm.

Table 1 Demographics of patients with Thy3f nodules and healthy individuals, concentrations of total L-EVs and L-EV subpopulations expressing cancer markers

	Age (years), median (i.q.r.)	Sex (M:F)	BMI (kg/m ²), median (i.q.r.)	Nodule size (mm), median (i.q.r.)	Total L-EV/ml, median (i.q.r.)	CXCR7 L-EV/ ml, median (i.q.r.)	CD147 L-EV/ ml, median (i.q.r.)	SDC4 L-EV/ml, median (i.q.r.)	EpCAM L-EV/ ml, median (i.q.r.)
Healthy controls (n = 16)	48 (25–75)	6:10	24.3 (21.2– 33)	–	1.12 × 10 ⁸ (0.95–1.30 × 10 ⁸)	1.01 × 10 ⁸ (0.86–1.16 × 10 ⁸)	1.51 × 10 ⁸ (1.27–1.91 × 10 ⁸)	1.36 × 10 ⁸ (1.20–1.80 × 10 ⁸)	3.45 × 10 ⁷ (2.56–4.24 × 10 ⁷)
Non-cancer Thy3f thyroid nodules (n = 14)	49.5 (24–73)	6:8	24.97 (20.5–38.2)	28 (4–60)	1.99 × 10 ⁸ (1.61–3.21 × 10 ⁸)	1.82 × 10 ⁸ (1.46–2.90 × 10 ⁸)	2.30 × 10 ⁸ (1.83–2.76 × 10 ⁸)	2.16 × 10 ⁸ (1.74–2.56 × 10 ⁸)	5.57 × 10 ⁷ (4.40–6.69 × 10 ⁷)
Cancer Thy3f thyroid nodules (n = 14)	46.3 (28–72)	4:10	25.3 (23.1– 28)	19 (2–56)	2.29 × 10 ⁸ (1.58–3.79 × 10 ⁸)	2.09 × 10 ⁸ (1.44–2.74 × 10 ⁸)	2.28 × 10 ⁸ (1.51–2.94 × 10 ⁸)	2.37 × 10 ⁸ (1.64–2.95 × 10 ⁸)	5.57 × 10 ⁷ (4.55–8.90 × 10 ⁷)
P value (ANOVA)	0.256	0.583	0.325	0.389	< 0.001	< 0.001	0.017	0.006	< 0.001

i.q.r., interquartile range; HC, healthy control; L-EV, large extracellular vesicle; cancer markers: epithelial marker: EpCAM, epithelial cell adhesion molecule; cancer markers: CXCR7, atypical chemokine receptor type 7; CD147, extracellular matrix metalloproteinase inducer; SDC4 syndecan-4.

Results

Patient characteristics

A total of 42 patients with Thy3f nodules and 16 HCs were included in this study. The final postoperative histopathological diagnoses of the patients were benign in 22: hyperplastic nodules in 10 of 22 (45%), follicular adenoma in 8 of 22 (36%), NIFTP in 4 of 22 (18%); 20 (48%) patients had thyroid cancer. A summary of patient and tumour characteristics is presented in [Table 1](#) and [Table S1](#).

Total and subpopulations of plasma L-EVs are elevated in patients with indeterminate thyroid nodules versus healthy controls

The concentrations of total plasma L-EVs were significantly higher in patients with cancerous and non-cancer Thy3f nodules compared with HCs ($P < 0.001$). Total plasma L-EV concentrations could differentiate patients with Thy3f nodules from HCs with AUC = 0.9444 (95% c.i. 0.8759 to 1.000, $P < 0.001$). Sensitivity and specificity were 92.6% (95% c.i. 76.63 to 98.68) and 81.2% (95% c.i. 56.99 to 93.41) respectively at a cut-off of 1.36×10^8 L-EVs/ml ([Fig. 1c, d](#)).

Plasma concentrations of L-EVs expressing surface markers CXCR7 ($P < 0.001$), CD147 ($P = 0.001$), SDC4 ($P = 0.03$) and EpCAM ($P < 0.001$) were higher in patients suffering from both benign and malignant Thy3f nodules compared with HCs ([Fig. 2a–d](#)). Total and subpopulation concentrations of plasma L-EVs did not discriminate between non-cancer and cancer Thy3f nodules.

Differentially expressed circulating L-EV miRNAs in patients with cancerous compared with non-cancerous Thy3f nodules

NGS of EV miRNAs yielded an average 24.12 million reads per sample. The average alignment ratio to the reference human genome was 60.99%. Percentage of clean tag reads ranged from 74.96 to 93.54%. NGS detected 650 miRNAs across all 20 samples; 120 miRNAs were exclusive to Thy3f cancer patients, 90 were exclusive to Thy3f non-cancer patients and 32 exclusive to HCs. A total of 234 miRNAs were common to all groups ([Fig. 3a, b](#)).

Comparing cancer versus non-cancer Thy3f nodule patients, six miRNAs were significantly differentially expressed. One was upregulated, mir-195-3p ($\log_2FC = 20.7$, $P < 0.001$), and five were downregulated: mir-3176 ($\log_2FC = -23.6$, $P < 0.001$), mir-205-5p ($\log_2FC = -23.0$, $P < 0.001$), novel-hsa-mir-208-3p ($\log_2FC = -21.9$, $P < 0.001$), mir-3529-3p ($\log_2FC = -11.5$, $P = 0.01$) and let-7i-3p

($\log_2FC = -9.1$, $P = 0.02$) ([Fig. 3c](#)). Principal component analysis of miRNA sequencing data is shown in [Fig. S1](#). Comparisons between Thy3f groups and HCs are in [Fig. S6](#) and [Table S2](#), and mRNA targets for differentially expressed miRNAs between patients with cancer/non-cancer Thy3f nodules in [Figs S8–12](#).

Differentially expressed circulating L-EV proteins in patients with cancerous compared with non-cancerous Thy3f nodules

A total of 1034 proteins were identified across all 32 samples. From the top 20 EV proteins reported in Vesiclepedia, an online EV molecular data repository²⁴, 15 were identified in our samples. The top five are: β -actin, flotillin 1, annexin A2, tetraspanin CD9 (CD9), and tetraspanin CD81 (CD81). Only β -actin was expressed across all 32 samples, while CD81 was expressed in the least number of samples (24 of 32). Principal component analysis ([Fig. 4a](#)) and unsupervised hierarchical clustering ([Fig. 4b](#)) showed HCs tightly clustered, while cancerous and non-cancer Thy3f nodules are interspersed. The Venn diagram ([Fig. 4d](#)) demonstrates 17 proteins expressed only in Thy3f cancer patients, 36 in Thy3f non-cancer patients, while 198 were exclusive to HCs; 612 proteins were common to all groups. Differential expression analysis showed three proteins significantly overexpressed in cancerous Thy3f nodules compared with non-cancer: kallikrein-related peptidase 11 (KLK11) ($\log_2FC = 12$; $P = 0.001$), α -1-acid glycoprotein 2 (A1AG2) ($\log_2FC = 2$; $P = 0.007$) and small integral membrane protein 1 (SMIM1) ($\log_2FC = 2$, $P = 0.04$). Significantly underexpressed were 20 proteins. The most underexpressed were chemokine (C-X-C motif) ligand 7 (CXCL7), tubulin β -1 chain (TBB1), actinin α -1 (ACTN1) and binding immunoglobulin protein (BIP) ([Fig. 4c](#)).

Discussion

This study explored the potential of circulating L-EVs as surrogate diagnostic biomarkers for indeterminate Thy3f thyroid nodules. Two novel findings are, first, a multi-platform omics approach identified several candidate L-EV miRNA and protein biomarkers that could potentially distinguish between patients with non-cancer and cancer Thy3f nodules. With respect to the cancer group, the upregulation of mir-195-3p, KLK11, A1AG2, SMIM1, and the downregulation of mir-3176, mir-205-5p, novel-hsa-mir-208-3p, mir-3529-3p and let-7i-3p, CXCL7, TBB1, ACTN1 and BIP were identified compared with the non-cancer

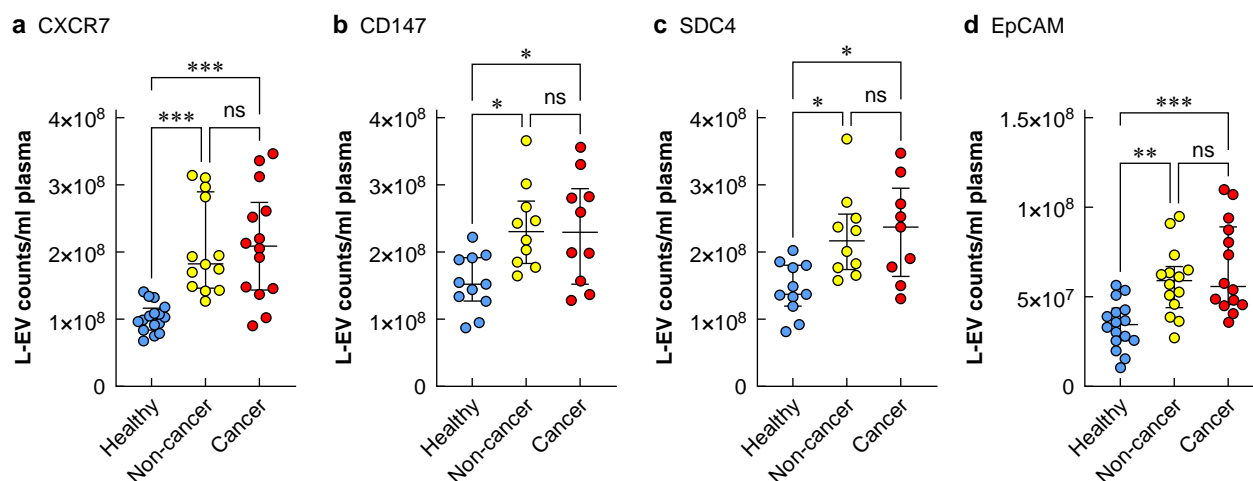


Fig. 2 Concentrations of L-EVs expressing CXCR7, CD147, SDC4 and EpCAM are elevated in plasma of patients with indeterminate Thy3f thyroid nodules compared with healthy controls.

L-EVs expressing: **a** CXCR7, **b** CD147, **c** SDC4 and **d** EpCAM measured in patients with cancer and non-cancer Thy3f nodules and healthy controls. Statistical analysis was tested using the Kruskal–Wallis test. Statistical significance was set at $P \leq 0.05$ (two-sided). Data are presented as median and interquartile ranges. *** $P < 0.001$, ** $P < 0.01$, * $P \leq 0.05$, ns $P > 0.05$. L-EV, large extracellular vesicle; CXCR7, atypical chemokine receptor type 7; CD147, extracellular matrix metalloproteinase inducer; SDC4, syndecan-4; EpCAM, epithelial cell adhesion molecule; ns, non significant.

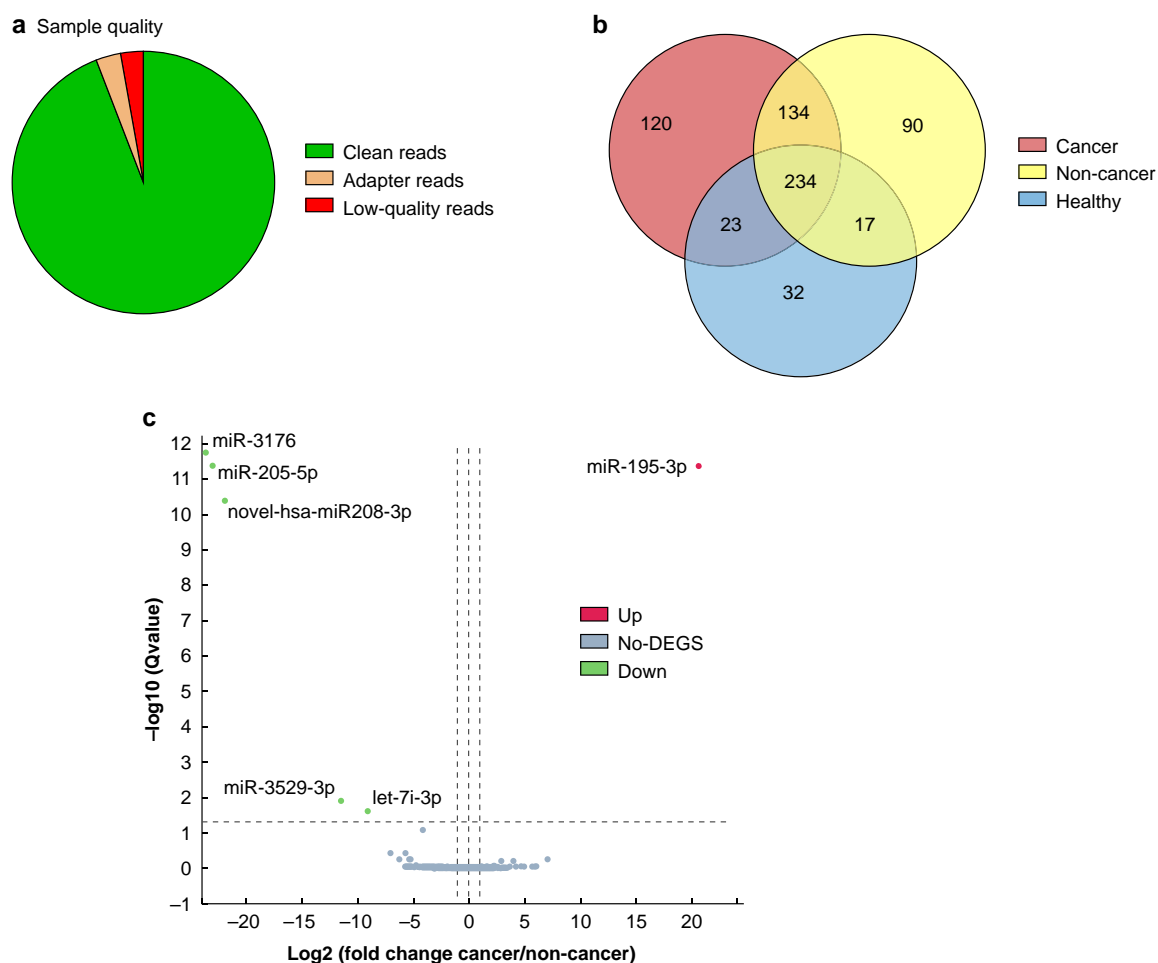


Fig. 3 L-EV miRNA sequencing

a Quality of plasma L-EV miRNA next generation sequencing showing ~95% clean reads from total sequenced reads. **b** Intersections between miRNAs identified in healthy controls (blue), patients with non-cancer (yellow) and cancer (red) Thy3f nodules are represented in the Venn diagram; the numbers represent the miRNAs identified in the respective group. **c** Volcano plot of differentially expressed miRNAs in patients with cancer versus non-cancer Thy3f nodules. The criteria for significant differential expression in DESeq2 was set at false discovery rates < 0.05 and a fold change threshold, $-1 > \log_2 FC > 1$. All miRNA sequencing data was analysed on the Dr Tom data analysis portal (BGI, Hong Kong). DEGS, differentially expressed genes/micro-RNAs; L-EV, large extracellular vesicle; miRNA, microRNA.

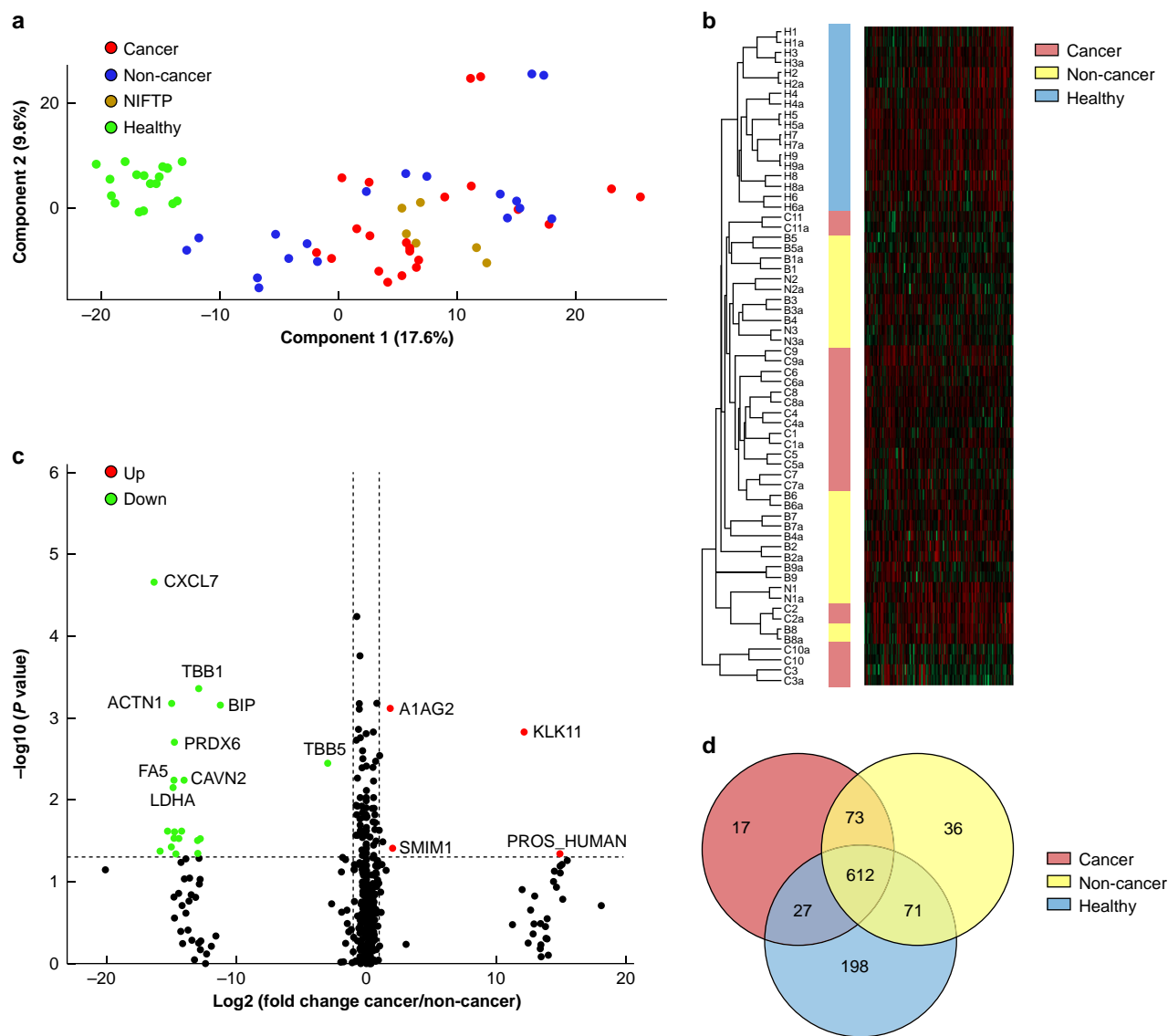


Fig. 4 L-EV proteomics

a Principal component analysis clustering samples based on their protein expression profiles. **b** Heatmap generated by unsupervised hierarchical clustering depicting a colour scale reflecting protein abundance. Horizontal rows indicate 34 independent L-EV samples (12 cancer and 12 non-cancer Thy3f samples, and 10 HCs). Vertical columns indicate the proteins identified by mass spectrometry ($n = 1034$ proteins). **c** Volcano plots of the differentially expressed proteins in L-EVs of patients with cancer compared with non-cancer Thy3f nodules. Statistical significance was tested using the Kruskal–Wallis test $P < 0.05$ and a fold change threshold, $-1 > \log_2 \text{FC} > 1$. **d** Venn diagram demonstrating intersections between proteins identified within the respective groups. PCA and heatmap were generated using Perseus software⁴¹, and Venn diagrams were created in Venny (<https://bioinfogp.cnb.csic.es/tools/venny/>). NIFTP, non-invasive follicular thyroid neoplasm with papillary like nuclear features; HC, healthy control; L-EV, large extracellular vesicle; PCA, principal component analysis.

group. Second, the concentrations of total and subpopulations of tumour-related plasma L-EVs were significantly higher in all patients with Thy3f nodules compared with HCs, with a high AUC. Similar findings have been shown in our laboratory where total L-EV concentrations were higher in benign and malignant colorectal polyps compared with HCs and are potential biomarkers for colorectal cancer screening and diagnosis²⁵.

To our knowledge, this is the first study investigating circulating EVs as diagnostic biomarkers of Thy3f nodules. Previous literature mainly focused on circulating small extracellular vesicles/exosomes (sEVs) as diagnostic or prognostic biomarkers for PTC^{26–32}. Unlike Thy3f nodules, PTCs can be confidently diagnosed on cytopathology in most patients based on their nuclear features¹. Moving forward, the identified biomarkers from this study will serve as candidates for validation on a larger patient

cohort using clinically established techniques such as polymerase chain reaction (PCR) and enzyme-linked immunosorbent assay (ELISA) for miRNA and proteins respectively. These techniques are in routine use in clinical laboratories, thus not needing specialized or centralized facilities. Furthermore, sEVs rather than L-EVs were the focus of previous research in the context of thyroid cancer biomarkers^{26–32}. L-EV isolation is easier than sEVs, which require ultracentrifugation at very high speeds, whereas L-EVs can be isolated by benchtop centrifuges at vastly lower speeds. In addition, L-EVs potentially carry a broader range of cargo molecules, owing to their larger size, as well as representative membrane markers, owing to their cell membrane origin³³.

Previous studies of sEVs showed that a panel of five miRNAs could discriminate follicular adenoma (FA) from FTC with an AUC of 0.924³⁴, while another study³⁵ identified two miRNAs of the

Let-7 family (Let-7f and Let-7d) to be overexpressed in a subgroup of plasma sEVs expressing thyroid peroxidase (TPO) that potentially can discriminate FA from FTC^{35,36}. Despite this, these studies only compared FA and FTC, thus these findings may not translate to clinical practice as this dichotomy does not represent the differentials of Thy3f nodules' final histopathology, which also include hyperplastic nodules, FV-PTCs (the most common benign and malignant diagnoses of Thy3f nodules) and NIFTPs³⁷.

In this work, hsa-mir-195-3p was significantly upregulated in plasma L-EVs of Thy3f cancer patients, similar to previous work showing its upregulation in serum of patients with well differentiated thyroid cancer (WDTC) compared with FA³⁸. Paradoxically, expression levels of hsa-mir-195-3p were down-regulated in WDTC tissue compared with FA³⁸. Together with our findings, this may indicate that hsa-mir-195-3p is selectively packaged and secreted from thyroid cancer cells into the blood-stream enclosed in EVs. Given its demonstrated pro-tumourigenic roles in cancer signalling pathways, including retinoblastoma-early region 2 binding factor and phosphatidylinositol 3-kinase pathways³⁹, hsa-mir-195-3p has strong potential as a relevant diagnostic biomarker for cancer in patients with Thy3f nodules.

KLK11 was significantly overexpressed in circulating L-EVs of Thy3f cancer compared with non-cancer patients. KLK11 has been implicated in carcinogenesis and is upregulated in ovarian, prostate, lung and rectal cancers⁴⁰. In a recent study, KLK11 mRNA levels were reported to be overexpressed in thyroid cancer compared with adjacent normal thyroid tissues, while its silencing in PTC cell lines inhibited proliferation, migration and invasiveness⁴¹.

Circulating L-EVs from Thy3f cancer patients had higher protein expression of A1AG2. Like the related A1AG1, it is an acute-phase plasma protein predominantly expressed in hepatocytes and upregulated in cancers including thyroid, hepatocellular and colorectal^{42–44}. Recently, A1AG2 was identified by mass spectrometry as one of the top three upregulated proteins in PTC compared with normal thyroid tissues⁴². This protein has also been previously identified in plasma EVs⁴⁵. The related A1AG1 is listed as a plasma and urinary EV protein in ExoCarta, an online EV database⁴⁶. Another upregulated L-EV protein in patients with cancer over non-cancer Thy3f nodules is SMIM1, a conserved small protein with a role in red blood cell development⁴⁷. A study characterizing EVs from 60 cell lines⁴⁸ detected SMIM1 in EVs isolated from eight cancer cell lines, as well as in EVs isolated from human plasma⁴⁹, breast milk and seminal fluid²⁴. SMIM1 is overexpressed in many cancers, with thyroid cancer showing the highest expression by immunohistochemistry⁵⁰. Interestingly, in the present study, β -actin was the only protein expressed in all L-EV samples as identified by proteomics and thus may serve as a generic marker for L-EVs.

This study exhibits many strengths that underscore its significance. Noteworthy attributes include its focus on a critical clinical matter, the use of clinical patient samples, a well matched HC group, well established methods of isolating and analysing L-EVs, and the identification of promising candidate L-EV biomarkers with the potential to distinguish between cancer and non-cancer Thy3f nodules. A liquid biopsy that could identify cancerous nodules without the need for diagnostic surgery would be of significant clinical relevance¹. This would help reduce exposure to undue risks and potential complications of diagnostic surgeries. L-EVs are a promising diagnostic modality that can be translated to clinical use owing to their stability and relative ease of isolation²⁵.

Despite its strengths, it is important to acknowledge that this study is in its initial discovery phase and the sample size remains

relatively small. This is not unprecedented in omics feasibility studies that are usually tailored to identify potential biomarkers for further validation^{31,32,51}. The variety of histological subtypes of nodules included might introduce heterogeneity to this study, which may limit the power of conclusions drawn. However, excluding some Thy3f nodules' differential diagnoses may introduce a selection bias not reflective of the range of diagnoses. Further work will require larger cohorts accounting for the breadth of Thy3f histological outcomes. Additionally, L-EV biomarkers were measured in total circulating L-EVs which are indeed a pool shed from all body organs⁵², thus some L-EVs may not be thyroid tumour derived. As such, further work is required to investigate the underlying biology of the identified markers. However, biomarkers may originate from cancer cells, cells in the tumour microenvironment (such as stromal cells, blood vessels, immune cells) or as a result of the host's immune response to cancer or other systemic processes triggered by the presence of the cancer^{52–54}. Hence specific L-EV biomarkers that are consistently differentially expressed in Thy3f cancer patients could still be used as a tumour fingerprint⁵³ and remain valuable even if not directly derived from cancer cells³¹. This is reinforced by the fact that the only EV liquid biopsy-based cancer diagnostic tests that have reached clinical application use total EVs including ExoDx™ Lung (ALK) and ExoDx Prostate IntelliScore (EPI), which analyse mRNAs extracted from total EVs as biomarkers for non-small cell lung cancer and prostate cancer respectively, with high sensitivity and specificity^{55,56}. In terms of costs, the miRNA and protein profiling of plasma L-EVs currently stand at a fraction of the cost of the commercially available molecular tests of fine needle aspiration material⁵⁷. As the test moves into the validation phase with clinically established techniques, a much greater cost reduction is anticipated.

Funding

University College London Hospitals Charity, Charity Number: 1165398 (UCLH Charity) (grant award number 534982), N.M.A. is fully funded by the Egyptian Cultural Affairs and Missions sector (grant award number MM42/19). Consumables of this work were funded by UCLH Charity (grant award number 534982) and the Egyptian Cultural Affairs and Missions' sector (award number MM42/19).

Acknowledgements

The authors thank the patients and volunteers who have participated in this study. Special thanks to Dr Michael Richard Lynch for his generous donation to UCLH Charity that helped fund this work. The authors also thank UCLH Charity and the Egyptian Cultural Affairs and Missions' sector for funding N.M.A.'s PhD scholarship and this project. The authors acknowledge the BJS Academy for awarding this study the BJS prize for best submitted manuscript at the European Society of Endocrine Surgery (ESES) meeting in Rome, Italy, May 2024, as judged by the BJS editor-in-chief and the chairman of the research committee of the ESES (conference abstract: <https://doi.org/10.1093/bjs/znac104.014>) after being nominated for the BJS prize session. Laboratory infrastructure for the work was provided by ICS, UCL.

Disclosure

The authors declare no conflict of interest.

Supplementary material

Supplementary material is available at *BJS Open* online.

Data availability

The data that support the findings of this study are available on request from the corresponding author.

Author contributions

Nada M. Ahmed (Conceptualization, Methodology, Investigation, Visualization, Project administration, Writing—original draft, Writing—review & editing), Mohammad M.R. Eddama (Conceptualization, Methodology, Visualization, Funding acquisition, Project administration, Supervision, Writing—review & editing), Kevin Beatson (Methodology, Investigation, Visualization, Writing—review & editing), Rijan Gurung (Conceptualization, Writing—review & editing), Jigisha Patel (Methodology, Investigation, Visualization, Writing—review & editing), Georges Iskandar (Writing—review & editing), Alaa Abdel-Salam (Writing—review & editing), Abdullah Al-Omar (Writing—review & editing), Richard Cohen (Funding acquisition, Writing—review & editing), Tarek Abdel-Aziz (Conceptualization, Funding acquisition, Supervision, Writing—review & editing), Lucie Clapp (Conceptualization, Funding acquisition, Project administration, Supervision, Writing—review & editing).

References

- Haugen BR, Alexander EK, Bible KC, Doherty GM, Mandel SJ, Nikiforov YE et al. 2015 American Thyroid Association management guidelines for adult patients with thyroid nodules and differentiated thyroid cancer: the American Thyroid Association guidelines task force on thyroid nodules and differentiated thyroid cancer. *Thyroid* 2016;**26**:1–133
- Cibas ES, Ali SZ. The 2017 Bethesda system for reporting thyroid cytopathology. *Thyroid* 2017;**27**:1341–1346
- Song JSA, Dmytriw AA, Yu E, Forghani R, Rotstein L, Goldstein D et al. Investigation of thyroid nodules: a practical algorithm and review of guidelines. *Head Neck* 2018;**40**:1861–1873
- Cross P, Chandra A, Giles T, Liverpool R, Johnson S, Kocjan G et al. Guidance on the reporting of thyroid cytology. The Royal College of Pathologists. https://www.rcpath.org/static/7d693ce4-0091-4621-97f79e2a0d1034d6/g089_guidance_on_reporting_of_thyroid_cytology_specimens.pdf. 2024
- Patel KN, Yip L, Lubitz CC, Grubbs EG, Miller BS, Shen W et al. The American Association of Endocrine Surgeons guidelines for the definitive surgical management of thyroid disease in adults. *Ann Surg* 2020;**271**:e21–e93
- Kandil E, Krishnan B, Noureldine SI, Yao L, Tufano RP. Hemithyroidectomy: a meta-analysis of postoperative need for hormone replacement and complications. *ORL J Otorhinolaryngol Relat Spec* 2013;**75**:6–17
- Agarwal S, Bychkov A, Jung CK. Emerging biomarkers in thyroid practice and research. *Cancers (Basel)* 2021;**14**:204
- De Rubis G, Rajeev Krishnan S, Bebawy M. Liquid biopsies in cancer diagnosis, monitoring, and prognosis. *Trends Pharmacol Sci* 2019;**40**:172–186
- Jimenez JJ, Jy W, Mauro LM, Soderland C, Horstman LL, Ahn YS. Endothelial cells release phenotypically and quantitatively distinct microparticles in activation and apoptosis. *Thromb Res* 2003;**109**:175–180
- Piccin A, Murphy C, Eakins E, Kunde J, Corvetta D, Di Pierro A et al. Circulating microparticles, protein C, free protein S and endothelial vascular markers in children with sickle cell anaemia. *J Extracell Vesicles* 2015;**4**:28414
- Elzanowska J, Semira C, Costa-Silva B. DNA in extracellular vesicles: biological and clinical aspects. *Mol Oncol* 2020;**15**:1701–1714
- Qiu ZL, Wei WJ, Sun ZK, Shen CT, Song HJ, Zhang XY et al. Circulating tumor cells correlate with clinicopathological features and outcomes in differentiated thyroid cancer. *Cell Physiol Biochem* 2018;**48**:718–730
- Garcia-Romero N, Esteban-Rubio S, Rackov G, Carrión-Navarro J, Belda-Iniesta C, Ayuso-Sacido A. Extracellular vesicles compartment in liquid biopsies: clinical application. *Mol Aspects Med* 2018;**60**:27–37
- Enderle D, Spiel A, Coticchia CM, Berghoff E, Mueller R, Schlumpberger M et al. Characterization of RNA from exosomes and other extracellular vesicles isolated by a novel spin column-based method. *PLoS One* 2015;**10**:e0136133
- Committee on the Review of Omics-Based Tests for Predicting Patient Outcomes in Clinical Trials, Board on Health Care Services, Board on Health Sciences Policy, Institute of Medicine. In: Micheel CM, Nass SJ, Omenn GS (eds). *Evolution of Translational Omics: Lessons Learned and the Path Forward*. Washington, DC: National Academies Press (US), 2012
- Lucien F, Gustafson D, Lenassi M, Li B, Teske JJ, Boilard E et al. MIBlood-EV: minimal information to enhance the quality and reproducibility of blood extracellular vesicle research. *J Extracell Vesicles* 2023;**12**:e12385
- de Rond L, van der Pol E, Hau CM, Varga Z, Sturk A, van Leeuwen TG et al. Comparison of generic fluorescent markers for detection of extracellular vesicles by flow cytometry. *Clin Chem* 2018;**64**:680–689
- Welsh JA, Van Der Pol E, Arkesteijn GJA, Bremer M, Brisson A, Coumans F et al. MIFlowCyt-EV: a framework for standardized reporting of extracellular vesicle flow cytometry experiments. *J Extracell Vesicles* 2020;**9**:1713526
- Kent WJ, Sugnet CW, Furey TS, Roskin KM, Pringle TH, Zahler AM et al. The human genome browser at UCSC. *Genome Res* 2002;**12**:996–1006
- Van Deun J, Mestdagh P, Agostinis P, Akay Ö, Anand S, Anckaert J et al. EV-TRACK: transparent reporting and centralizing knowledge in extracellular vesicle research. *Nat Methods* 2017;**14**:228–232
- Tyanova S, Temu T, Sinitcyn P, Carlson A, Hein MY, Geiger T et al. The Perseus computational platform for comprehensive analysis of (prote)omics data. *Nat Methods* 2016;**13**:731–740
- Oliveros JC. VENNY. An interactive tool for comparing lists with Venn diagrams. Venny 2.1.0. <https://bioinfogp.cnb.csic.es/tools/venny>. (accessed 30 October 2024)
- Howard J, Wynne K, Moldenhauer E, Clarke P, Maguire C, Bollard S et al. A comparative analysis of extracellular vesicles (EVs) from human and feline plasma. *Sci Rep* 2022;**12**:10851
- Chitti SV, Gummadi S, Kang T, Shahi S, Marzan AL, Nedeva C et al. Vesiclepedia 2024: an extracellular vesicles and extracellular particles repository. *Nucleic Acids Res* 2024;**52**:D1694–D16D8
- Eddama MMR, Gurung R, Fragkos K, Lorgelly P, Cohen R, Loizidou M et al. The role of microvesicles as biomarkers in the screening of colorectal neoplasm. *Cancer Med* 2022;**11**:2957–2968
- Capriglione F, Verrienti A, Celano M, Maggisano V, Sponziello M, Pecce V et al. Analysis of serum microRNA in exosomal vehicles of papillary thyroid cancer. *Endocrine* 2022;**75**:185–193

27. Chen W, Li G, Li Z, Zhu J, Wei T, Lei J. Evaluation of plasma exosomal miRNAs as potential diagnostic biomarkers of lymph node metastasis in papillary thyroid carcinoma. *Endocrine* 2022;**75**:846–855
28. Dai D, Tan Y, Guo L, Tang A, Zhao Y. Identification of exosomal miRNA biomarkers for diagnosis of papillary thyroid cancer by small RNA sequencing. *Eur J Endocrinol* 2019;**182**:111–121
29. Zou X, Gao F, Wang ZY, Zhang H, Liu QX, Jiang L et al. A three-microRNA panel in serum as novel biomarker for papillary thyroid carcinoma diagnosis. *Chin Med J (Engl)* 2020; **133**:2543–2551
30. Delcorte O, Craps J, Mahibullah S, Spourquet C, D'Auria L, Van Der Smissen P et al. Two miRNAs enriched in plasma extracellular vesicles are potential biomarkers for thyroid cancer. *Endocr Relat Cancer* 2022;**29**:389–401
31. Haigh T, Beattie H, Wade MA, England J, Kuvshinov D, Karsai L et al. The use of tissue-on-chip technology to focus the search for extracellular vesicle miRNA biomarkers in thyroid disease. *Int J Mol Sci* 2023;**25**:71
32. Ye W, Deng X, Fan Y. Exosomal miRNA423–5p mediated oncogene activity in papillary thyroid carcinoma: a potential diagnostic and biological target for cancer therapy. *Neoplasma* 2019;**66**:516–523
33. Soukup J, Moško T, Kerešič S, Holada K. Large extracellular vesicles transfer more prions and infect cell culture better than small extracellular vesicles. *Biochem Biophys Res Commun* 2023;**687**:149208
34. Li G, Wang H, Zhong J, Bai Y, Chen W, Jiang K et al. Circulating small extracellular vesicle-based miRNA classifier for follicular thyroid carcinoma: a diagnostic study. *Br J Cancer* 2024;**130**:925–933
35. Zabegina L, Nazarova I, Knyazeva M, Nikiforova N, Slyusarenko M, Titov S et al. MiRNA let-7 from TPO(+) extracellular vesicles is a potential marker for a differential diagnosis of follicular thyroid nodules. *Cells* 2020;**9**:1917
36. Karlsson M, Zhang C, Méar L, Zhong W, Digre A, Katona B et al. A single-cell type transcriptomics map of human tissues. *Sci Adv* 2021;**7**:eabh2169
37. Yaprak Bayrak B, Erucar AT. Malignancy rates for Bethesda III and IV thyroid nodules: a retrospective study of the correlation between fine-needle aspiration cytology and histopathology. *BMC Endocr Disord* 2020;**20**:48
38. Świrta JS, Wątor G, Seweryn M, Kapusta P, Barczyński M, Wołkow P. Expression of micro-ribonucleic acids in thyroid nodules and serum to discriminate between follicular adenoma and cancer in patients with a fine needle aspiration biopsy classified as suspicious for follicular neoplasm: a preliminary study. *Adv Clin Exp Med* 2023;**32**:997–1007
39. Dasgupta I, Chatterjee A. Recent advances in miRNA delivery systems. *Methods Protoc* 2021;**4**:10
40. Mavridis K, Scorilas A. Prognostic value and biological role of the kallikrein-related peptidases in human malignancies. *Future Oncol* 2010;**6**:269–285
41. Ni T, Zhao RH, Wu JF, Li CY, Xue G, Lin X. KLK7, KLK10, and KLK11 in papillary thyroid cancer: bioinformatic analysis and experimental validation. *Biochem Genet* 2024; doi:10.1007/s10528-024-10679-8
42. Wei W, Wu Y, Chen D-D, Song Y, Xu G, Shi Q et al. Proteomics profiling for the global and acetylated proteins of papillary thyroid cancers. *Proteome Sci* 2023;**21**:6
43. Fang T, Cui M, Sun J, Ge C, Zhao F, Zhang L et al. Orosomucoid 2 inhibits tumor metastasis and is upregulated by CCAAT/enhancer binding protein β in hepatocellular carcinomas. *Oncotarget* 2015;**6**:16106–16119
44. Zhang X, Xiao Z, Liu X, Du L, Wang L, Wang S et al. The potential role of ORM2 in the development of colorectal cancer. *PLoS One* 2012;**7**:e31868
45. Mao K, Tan Q, Ma Y, Wang S, Zhong H, Liao Y et al. Proteomics of extracellular vesicles in plasma reveals the characteristics and residual traces of COVID-19 patients without underlying diseases after 3 months of recovery. *Cell Death Dis* 2021;**12**:541
46. Keerthikumar S, Chisanga D, Ariyaratne D, Al Saffar H, Anand S, Zhao K et al. ExoCarta: a web-based compendium of exosomal cargo. *J Mol Biol* 2016;**428**:688–692
47. Nylander A, Leznicki P, Vidovic K, High S, Olsson ML. SMIM1, carrier of the vel blood group, is a tail-anchored transmembrane protein and readily forms homodimers in a cell-free system. *Biosci Rep* 2020;**40**:BSR20200318
48. Hurwitz SN, Rider MA, Bundy JL, Liu X, Singh RK, Meckes DG Jr. Proteomic profiling of NCI-60 extracellular vesicles uncovers common protein cargo and cancer type-specific biomarkers. *Oncotarget* 2016;**7**:86999–87015
49. Al Kaabi A, Traupe T, Stutz M, Buchs N, Heller M. Cause or effect of arteriogenesis: compositional alterations of microparticles from CAD patients undergoing external counterpulsation therapy. *PLoS One* 2012;**7**:e46822
50. Sjöstedt E, Zhong W, Fagerberg L, Karlsson M, Mitsios N, Adori C et al. An atlas of the protein-coding genes in the human, pig, and mouse brain. *Science* 2020;**367**:eaay5947
51. Perng W, Aslibekyan S. Find the needle in the haystack, then find it again: replication and validation in the 'omics era. *Metabolites* 2020;**10**:286
52. Klein EA, Richards D, Cohn A, Tummala M, Lapham R, Cosgrove D et al. Clinical validation of a targeted methylation-based multi-cancer early detection test using an independent validation set. *Ann Oncol* 2021;**32**:1167–1177
53. Yu S, Liu Y, Wang J, Guo Z, Zhang Q, Yu F et al. Circulating microRNA profiles as potential biomarkers for diagnosis of papillary thyroid carcinoma. *J Clin Endocrinol Metab* 2012;**97**:2084–2092
54. Connal S, Cameron JM, Sala A, Brennan PM, Palmer DS, Palmer JD et al. Liquid biopsies: the future of cancer early detection. *J Transl Med* 2023;**21**:118
55. Yu B, Du Q, Li H, Liu HY, Ye X, Zhu B et al. Diagnostic potential of serum exosomal colorectal neoplasia differentially expressed long non-coding RNA (CRNDE-p) and microRNA-217 expression in colorectal carcinoma. *Oncotarget* 2017;**8**:83745–83753
56. McKiernan J, Donovan MJ, Margolis E, Partin A, Carter B, Brown G et al. A prospective adaptive utility trial to validate performance of a novel urine exosome gene expression assay to predict high-grade prostate cancer in patients with prostate-specific antigen 2–10 ng/ml at initial biopsy. *Eur Urol* 2018;**74**:731–738
57. Uppal N, Collins R, James B. Thyroid nodules: global, economic, and personal burdens. *Front Endocrinol (Lausanne)* 2023;**14**:1113977